

Numerical simulations of laser ablated plumes using Particle-in-Cell (PIC) methods

FILIPPO GENCO AND AHMED HASSANEIN

Center for Materials Under Extreme Environment, School of Nuclear Engineering, Purdue University, West Lafayette, Indiana

(RECEIVED 3 October 2013; ACCEPTED 31 January 2014)

Abstract

Laser ablation of graphite materials in the presence of an external magnetic field is studied with the use of the newly developed HEIGHTS-PIC particle-in-cell code and compared with both theoretical and experimental results. Carbon plumes behavior controlled by a strong magnetic field is of interest to evaluate the plume shielding effects to protect the original exposed target from further damage and erosion. Since intense power deposition on plasma facing components is expected during Tokamaks loss of plasma confinement events such as disruptions, vertical displacements event, runaway electrons, or during normal operating conditions such as edge-localized modes, it is critical to better understand the evolving target plasma behavior for more accurate prediction of the potential damage created by these high-energetic dumps which may not be easily mitigated without loss of structural and functional performance of the plasma facing components. Numerical experiments have been performed to provide benchmarking conditions for the HEIGHTS-PIC simulation package originally designed to evaluate the erosion of the Tokamak surfaces, splashing of the melted/ablated-vaporized material, and transport into the bulk plasma with consequent plasma contamination. Evolving target plasma temperature and density are calculated and compared with measured reported values available into literature for similar conditions and show good agreement with the HEIGHTS-PIC package predictions.

Keywords: Carbon plume plasma; HEIGHTS; Laser absorption; Laser target interaction; Particle in Cell

INTRODUCTION

Laser ablation is a well-known method for removing material from a target surface whenever it is irradiated with a high intensity laser. The process of laser ablation involves a complex series of physical events starting from a rapid heating, possible phase change, and evaporation of the target forming a thin layer of very dense gas made of neutrals, electrons, and ions. As time progresses the formed plasma interacts with the incoming laser beam photons increasing its pressure and temperature rapidly. This interaction is so important that governs strongly the ablation rate (Genco & Hassanein, 2011; Harilal *et al.*, 2011). The plume in fact can become so dense that can hinder the laser radiation from reaching the target and effectively screening it from further damage. This phenomenon is similar to the one present in similar conditions during loss of plasma confinement during disruptions and off-normal Tokamak events. Even if the power fluxes

during such events are much lower in Tokamaks, still erosion, damage, and plasma contamination are actively studied and simulated in order to reduce the structural impact over the plasma facing components (Hassanein, 1996). The presence of the magnetic field and its orientation is successfully used to mitigate some aspects of such high energetic events. Carbon has been studied for many years as possible candidate of divertors and plasma facing components in Tokamaks and understanding its plasma plume evolution and shielding effects is still very important. Other studies using laser pulses interacting with an external magnetic field have pointed out the importance of the $\vec{J} \times \vec{B}$ force in effectively containing the plume propagation converting kinetic energy into thermal energy (Pathak & Chandy, 2009). All these aspects of the plasma plume are studied and analyzed using HEIGHTS-PIC package and showed good agreement with both theoretical and experimental available results.

THEORETICAL MODEL

The HEIGHTS-PIC two-dimensional simulation package has been developed using a novel approach for the

Address correspondence and reprint request to Filippo Genco, Center for Materials Under Extreme Environment, School of Nuclear Engineering, Purdue University, West Lafayette, Indiana 47907. E-mail: fgenco@purdue.edu

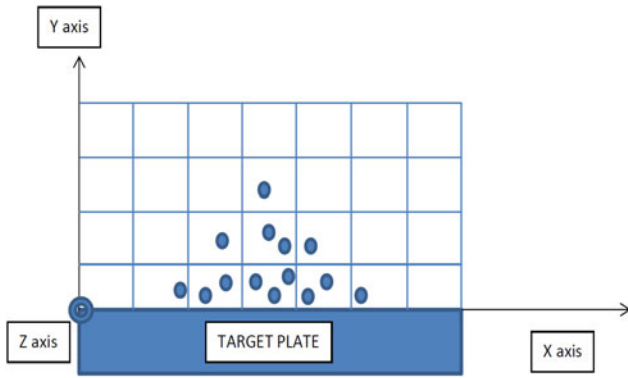


Fig. 1. (Color online) HEIGHTS-PIC modeling geometry.

Particle-in-Cell technique with the aim of detailed analysis of intense power deposition on target materials and the resulting erosion damage, for example, over plasma facing components in Tokamaks and plasma evolution over the divertor plate. HEIGHTS-PIC is a “full-particle” representation for the momentum and energy Lagrangian variables and follows the projection of the evolution of the plasma after impingement (Genco & Hassanein, 2011; 2014). The position of the expanding vapor front is evaluated following each time step and compared to the original position of the birth of particles as schematically illustrated in Figure 1.

One of the boundaries (the target surface) has a dynamical evolution and allows for the introduction of new generated sample particles as the material vaporizes. The sample particles or “super particles” are considered one-dimensional allowing them to be stacked along the X-axis and in layers along the Y-axis but having no dimension in this direction (Fig. 1). No map is used to transfer the properties from particles to the original grid as the conditions established by the ensemble of particles in a cell are evaluated producing the same effect inside the cell itself. The evolving characteristics of the particles inside the cells are assumed homogeneous throughout the cells. Diffusion due to the presence of a strong magnetic field is also considered and incorporated into the particle motion with possibility to include different starting diffusion coefficients and data obtained from experiments. The equations of conservation of mass, momentum, and energy are solved in two-dimensional representation (x - y plane) allowing for the plasma characteristics to be evaluated per each cell on the top of the target itself. The target heating by the laser beam is described by the equation:

$$\rho c_p \frac{\partial T}{\partial t} = \nabla \cdot (K \nabla T) + (1 - R) \alpha I_S e^{(-\alpha y)}, \quad (1)$$

where T is the temperature, c_p is the specific heat, ρ is the density, K is the thermal conductivity, R is the target reflectivity of laser photons, α is the graphite absorption, $I_S = I_0 \exp(-\int \kappa dy)$ with I_0 is maximum laser intensity, κ plasma absorption coefficient, and y is the axial coordinate.

In HEIGHTS-PIC, the solution of the transient heat transfer equations was developed with temperature and phase change dependent thermal properties (density, thermal conductivity, and specific heat). The surface temperature calculation requires the evaluation of the single portions of incident energy that go into conduction, melting, evaporation, and radiation. The kinetics of the evaporation provides the physical and mathematical connection between the out coming net particle flux from the surface and the surface temperature. Considering r as the radial distance in the plane x - z with origin in the center of the plate itself, the boundary condition at the target surface is expressed by:

$$F(r, t) = -K(T_v(r)) \frac{\partial T}{\partial z} + \rho(T_v(r)) L_v(T_v(r)) V(T_v(r)) + \sigma \epsilon (T_v^4(r) - T_0^4) \quad (2)$$

where $F(r, t)$ is the radial heat flux coming from the plasma, L_v is the heat of vaporization, $V(T_v)$ is the velocity of the receding surface, and $T_v = T(r, t)$. The velocity of the receding surface is typically a function of the instantaneous surface temperature and other materials parameters. The last term of the equation is the radiative heat transfer term. It contains T_0 , which is the temperature of the surroundings, σ is the Stefan-Boltzmann constant, and ϵ is material emissivity.

As the vapor starts building up and becomes thicker and thicker above the target surface, the vapor shielding of incoming laser power becomes more and more pronounced changing the boundary condition into:

$$-K \frac{\partial T}{\partial y}(0, t) = q_{GAS} + q_{RAD} - q_{EVAP} \quad (3)$$

where q_{GAS} is the net heat flux from the near-wall vapor cloud, q_{RAD} is the photon radiation heat flux absorbed at the material surface, and q_{EVAP} is the evaporation heat flux calculated from the enthalpy of evaporation for the material under investigation, i.e., carbon in this case. The evaporation flux is calculated using the Hertz-Knudsen-Langmuir theory of evaporation and condensation under non-equilibrium conditions (Hassanein *et al.*, 1981; 1982). As the laser pulse comes to an end, the plasma starts cooling down and starts its expansion phase. The expansion of the vapor/plasma into vacuum is then determined by solving the MHD equations for conservation of mass, momentum, and energy (4a) associated with Maxwell equations (4b):

$$\begin{aligned} \frac{\partial \rho}{\partial t} + \vec{\nabla} \cdot \rho \vec{V} &= 0 \\ \frac{\partial \rho \vec{V}_x}{\partial t} + \vec{\nabla} \cdot \rho V_x \vec{V} + \frac{\partial}{\partial x} \left(P + \frac{B^2}{2\mu_0} \right) - \frac{1}{\mu_0} \left(\vec{B} \vec{\nabla} \right) B_x &= F_x \\ \frac{\partial \rho \vec{V}_y}{\partial t} + \vec{\nabla} \cdot \rho V_y \vec{V} + \frac{\partial}{\partial x} \left(P + \frac{B^2}{2\mu_0} \right) - \frac{1}{\mu_0} \left(\vec{B} \vec{\nabla} \right) B_y &= F_y = 0 \end{aligned}$$

$$\frac{\partial \rho \vec{V}_z}{\partial t} + \vec{\nabla} \cdot \rho V_z \vec{V} - \frac{1}{\mu_0} (\vec{B} \cdot \vec{\nabla}) B_z = 0$$

$$\frac{\partial}{\partial t} \left\{ \rho e_i + \frac{\rho V^2}{2} + \frac{B^2}{2\mu_0} \right\} + \vec{\nabla} \cdot \left\{ \vec{V} \left(\rho e_i + \frac{\rho V^2}{2} \right) + \vec{P} \cdot \vec{V} - K \vec{\nabla} T_e + S_{Rad} + \frac{\vec{E} \times \vec{B}}{\mu_0} \right\} = Q_{Beam} \tag{4a}$$

$$\frac{\partial \vec{B}}{\partial t} = -\vec{\nabla} \times \vec{E}$$

$$\frac{1}{\mu_0} \vec{\nabla} \times \vec{B} = \vec{J}$$

$$\vec{\nabla} \cdot \vec{B} = 0$$

$$\vec{\nabla} \cdot \vec{E} = \rho_e$$

$$\vec{E} + \vec{V} \times \vec{B} = \frac{1}{\sigma} \vec{J}$$
(4b)

where ρ is the density, \vec{V} is the vapor velocity, P is the pressure, E is the energy, K is the vapor conductivity, Q_b is the incident photons flux from the incoming laser pulse, and Q_r is the radiation flux. The equation describing the vapor motion in a magnetic field is given by:

$$\rho \frac{\partial \vec{V}}{\partial t} = -\nabla P + \vec{J} \times \vec{B} \tag{5}$$

where $\vec{J} \times \vec{B}$ is the magnetic force. The vapor plasma, once it is ionized, moves freely along the magnetic field lines. More details of the model can be found in previous publications (Hassanein, 1994; Hassanein & Konkashbaev, 1995).

NUMERICAL SIMULATION

The performance of a graphite target irradiation was simulated numerically mimicking a ND:YAG laser operating with a Gaussian beam shape at its fundamental wavelength of 1064 nm with pulse energy of 400 mJ, total pulse duration of 30 ns with full width at half maximum of 10 ns. The laser spot size on the target has a diameter of 0.1784 cm (area of 2.5 mm²) with a laser total energy flux close to 16 J/cm² with intensity of 1.6 GW/cm². Plasma evolution was simulated up to 40 ns from the start of the laser beam. A magnetic field of 0.5 T was assumed perpendicular to the target. The number of super particles initially loaded into HEIGHTS-PIC was relatively low ($N = 20$) and the numerical grid used was made of 6 cells along the X-axis and 10 cells along the Y-axis for a total cell dimension of 0.0296 cm × 0.033 cm.

RESULTS AND DISCUSSION

The effect of the impinging laser onto the target surface and plasma energy absorption is described in Figures 2 and 3.

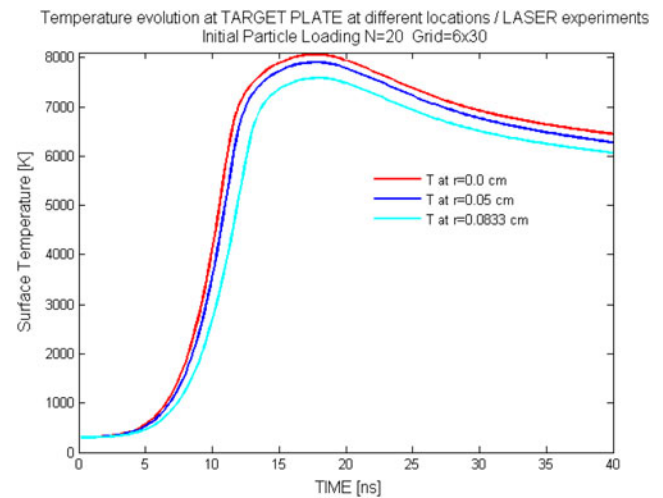


Fig. 2. (Color online) Evolution of the calculated target temperature along time at different locations.

The temperature of the target surface reaches its maximum around 8060 K at the center of the beam ($r = 0$) in the x - z plane and is lower for increasing values of the radius r , which follows the laser beam profile. This maximum temperature value is very close to recent work for similar laser energy flux (Bulgakova *et al.*, 2004).

The effective power flux reaching the surface changes rapidly with time. Given the temporal Gaussian evolution of the intensity of the laser beam, it is evident that initially all the energy goes into the target plate increasing its temperature. The value of laser reflectivity used is taken from (Bulgakova *et al.*, 2001; Malvezzi & Bloembergen, 1986) and provides the variation of carbon reflectivity as a function of the surface temperature. It is equal to $R = 0.21$ at the beginning ($T = 300$ K) and becomes very small at higher temperatures (less than 0.05 for $T > 6000$ K). When plasma starts being formed around 11 ns, the carbon plate has already reached a surface temperature close to 5000 K so that its reflectivity according to Bulgakova and Bulgakov (2001) is calculated roughly equal to 0.08 and rapidly diminishing.

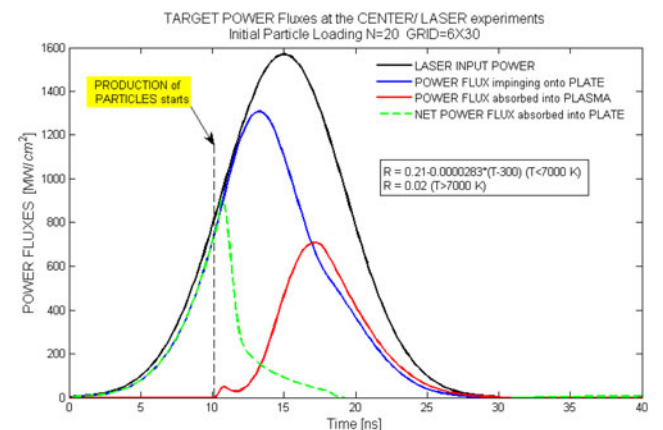


Fig. 3. (Color online) Power fluxes in the first instants of the laser pulse.

In fact, in the very first nanoseconds of the pulse, and up to the time in which the temperature in the target has been raised enough to vaporize the material and eject particles from the surface (i.e., 10.8 ns), the total laser power flux goes into the plate and it is fully absorbed (Fig. 3). As carbon plasma is formed and vapor particles are produced and emitted into the system, some of the incoming laser power flux starts being absorbed into the plasma itself through photon interaction, reducing the effective amount of power reaching the plate. As this phenomenon becomes more and more important, more and more energy is absorbed into the plume effectively screening the target for further damage. The direct laser intensity to target drops rapidly toward zero up to a point in which the target is totally screened from it and further erosion is eventually produced by the radiation only as shown in Figure 4.

The value of the maximum erosion calculated after one laser pulse (0.33 μm) is very close to the ones provided in the literature both theoretically and experimentally for similar conditions (Bulgakov & Bulgakova, 1999; Hoffman *et al.*, 2011). It is also very similar to the value of 0.40 μm predicted by the well-known and well benchmarked HEIGHTS-LPP package (Sizyuk *et al.*, 2006).

Looking at the integrated energy fluxes at the end of the pulse (Fig. 5), it can be seen that of the total energy provided (100%, blue line) only 22% is effectively absorbed into the plate while all the rest (78% black line) is absorbed into plasma (45%, cyan line) or reradiated back (33%, green line) This distribution of total energies is also very close to the one provided by other theoretical models (Bulgakova *et al.*, 2004).

Values of the electron density and temperature of the plasma are calculated along the entire mesh and for each time step. At 40 ns the profile of temperature close to the

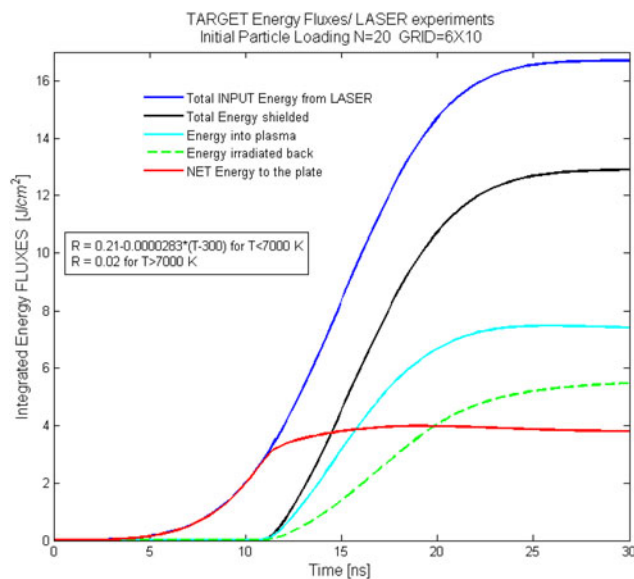


Fig. 5. (Color online) Calculated integrated energy fluxes of the system.

target still has a Gaussian shape. The peak of temperature is around 6.6 eV and drops with distance as expected (Harilal *et al.*, 1997). The comparison with experimental data for similar conditions is quite good given the experimental error of ±15% for the electron temperature (Fig. 6).

Electron density has a similar profile. The experimental values provided in the literature report at such close distance to target an error of the measurements around 50–60% for electron density (Hoffman *et al.*, 2011) so that the comparison can be considered fair (Fig. 7).

It should be pointed out, that HEIGHTS-PIC has, into the solution of the hydrodynamics equations, the implementation of the contribution of the magnetic force. As observed

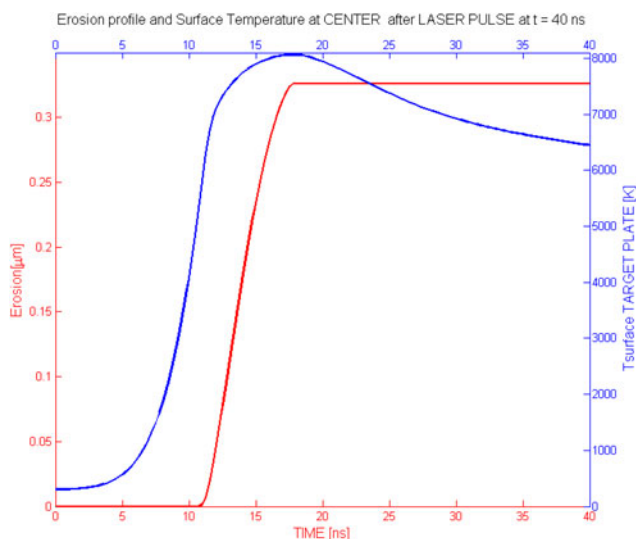


Fig. 4. (Color online) Calculated evolution of the erosion of the carbon target center along time and variation of maximum T surface at the center of the plate.

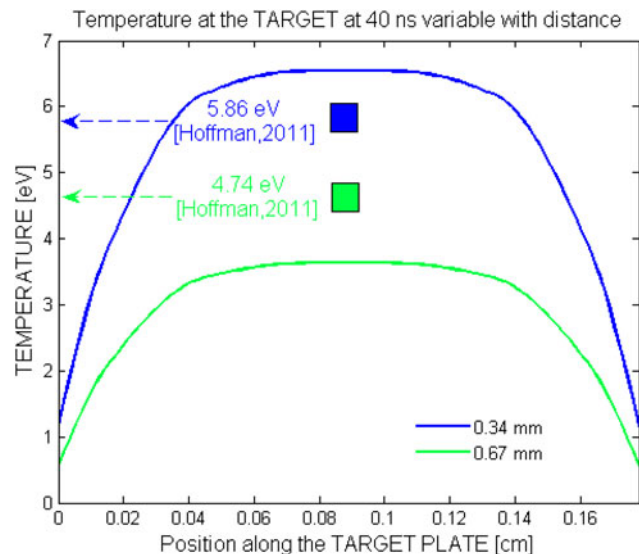


Fig. 6. (Color online) Calculated plasma temperature profiles close to the target at 40 ns and comparison with experimental data (Hoffman *et al.*, 2011).

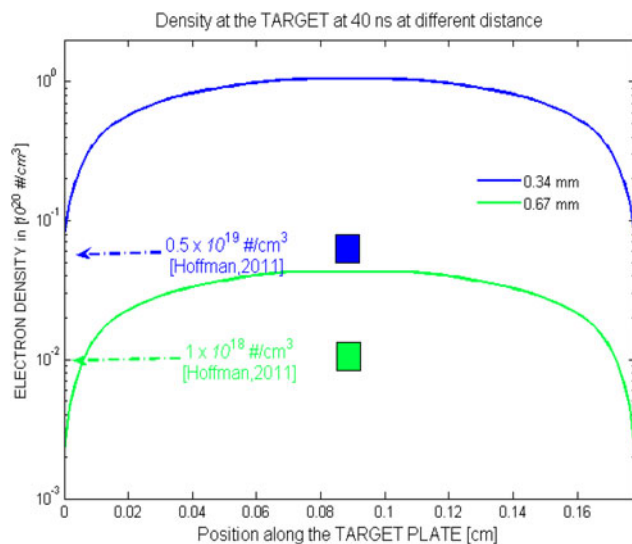


Fig. 7. (Color online) Calculated electron density profiles close to the target at 40 ns and comparison with experimental data (Hoffman *et al.*, 2011).

already (Pathak & Chandy, 2009; Neogi & Thareja, 2001) the presence of the $\vec{J} \times \vec{B}$ magnetic force changes the behavior of the plasma plume with respect to the one expanding for example into vacuum having a strong influence on the ionization characteristics as well as on the velocity of the plume itself. This translates for axial magnetic field as for HEIGHTS-PIC in a stronger confinement close to target.

Since some uncertainty still exists regarding the reflectivity of graphite exposed to laser pulse, Tokamak graphite has also been considered. The reflectivity of dense graphite has been estimated at room temperature around $R = 0.40$ to 0.29 while it appears that due to high porosity $R = 0.22$ (Semerok *et al.*, 2007) in Tokamaks; this value is also almost

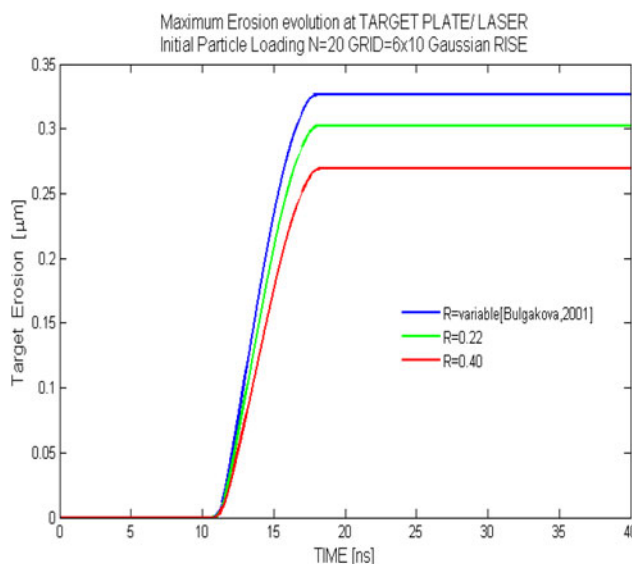


Fig. 8. (Color online) Calculated evolution of the erosion of the carbon target center along time with different values of the carbon reflectivity.

independent from surface temperature (Semerok *et al.*, 2007). For this reason, HEIGHTS-PIC was also run with $R = 0.22$ constant and $R = 0.40$ for the entire simulation in order to evaluate differences with the previous examined case. Particularly interesting are the profiles of erosion. In fact as shown in Figure 8 final erosions can be different according to which type of graphite reflectivity is used into the calculation.

With variable reflectivity the calculated erosion is more significant than the other two cases with constant reflectivity. In fact as soon as the temperature is elevated enough from the original 300 K, R tends to go down and becomes almost insignificant at high temperatures. Instead for the other two cases with R constant, since more energy is reflected back and eventually lost, less is the energy reaching the surface producing less erosion. So a more accurate evaluation of the behavior of reflectivity along with time under beam irradiation is critical in order to establish more accurate erosion and lifetime values.

CONCLUSION

In this work, HEIGHTS-PIC computer package has been modified and used to simulate carbon laser plasma evolution in the presence of magnetic field. The erosion profile and depth are in good agreement with the available experimental and theoretical data in the literature for similar conditions as well as the measurements of target temperature. While the evolution of plasma temperature is close to the experimental reported values, electron density seems to be a bit higher than what is measured. The presence of the magnetic field into the system changes the characteristics of the expansion of the plasma toward the vacuum and leads, due to Joule heating and higher confinement, to higher values of both temperature and density of the plasma with respect to the without magnetic field case. The screening effect that reduces the damage to the target plate is well described by HEIGHTS-PIC as well as the evolution of the carbon plume in its fundamental aspects.

ACKNOWLEDGEMENT

This work is partially supported by the US Department of Energy, Office of Fusion Energy Sciences.

REFERENCES

- BULGAKOV, A.V. & BULGAKOVA, N.M. (1999). Thermal model of pulsed laser ablation under the conditions of formation and heating of a radiation-absorbing plasma. *Quant. Electron.* **29**, 433–437.
- BULGAKOVA, N.M. & BULGAKOV, A.V. (2001). Pulsed laser ablation of solids: Transition from normal vaporization to phase explosion. *Appl. Phys. A* **73**, 199–208.
- BULGAKOVA, N.M., BULGAKOV, A.V. & BABICH, L.P. (2004). Energy balance of pulsed laser ablation: thermal model revised. *Appl. Phys. A* **79**, 1323–1326.

- GENCO, F. & HASSANEIN, A. (2011). Modeling of damage and lifetime analysis of plasma facing components during plasma instabilities in Tokamaks. *Fusion Sci. & Techn.* **60**, 339–343.
- GENCO, F. & HASSANEIN, A. (2014). Particle-in-Cell (PIC) methods in predicting materials behavior during high power deposition. *Laser Part. Beams*. <http://dx.doi.org/10.1017/S026303461400007X>.
- HARILAL, S.S., BINDHU, C.V., ISSAC, R.C., NAMPOORI, V.P.N. & VALLABHAN, C.P.G. (1997). Electron density & temperature measurements in a laser produced carbon plasma. *J. Appl. Phys.* **82**, 2140–2146.
- HARILAL, S.S., SIZYUK, T., HASSANEIN, A., CAMPOS, D., HOUGH, P. & SIZYUK, V. (2011). The effect of excitation wavelength on dynamics of laser-produced-plasmas. *J. Appl. Phys.* **109**, 063306.
- HASSANEIN, A. & KONKASHBAEV, I. (1995). Comprehensive model for disruption erosion in a reactor environment. *J. Nucl. Mater.* **220**, 244–248.
- HASSANEIN, A. (1994). Plasma disruption modeling and simulation. *Fusion Techn.* **26**, 532–539.
- HASSANEIN, A. (1996). Disruption damage to plasma-facing components from various plasma instabilities. *Fusion Techn.* **30**, 713–719.
- HASSANEIN, A., KULCINSKI, G.L. & WOLFER, W.G. (1981). Vaporization and melting of materials in fusion devices. *Nucl. Mater.* **103 & 104**, 311.
- HASSANEIN, A., KULCINSKI, G.L. & WOLFER, W.G. (1982). Dynamics of melting, evaporation, and resolidification of materials exposed to plasma disruptions. *J. Nucl. Mater.* **111 & 112**, 554.
- HOFFMAN, J., MOSCICKI, T. & SZYMANSKI, Z. (2011). The effect of laser wavelength on heating of ablated carbon plume. *Appl. Phys. A* **104**, 815–819.
- MALVEZZI, A.M. & BLOEMBERGEN, N. (1986). Time resolved picosecond optical measurements of laser-excited Graphite. *Phys. Rev. Lett.* **57**, 146–149.
- NEOGI, A. & THAREJA, R.K. (2001). Laser ablated carbon plume flow dynamics under magnetic field. *Appl. Phys. B* **72**, 231–235.
- PATHAK, K. & CHANDY, A. (2009). Laser ablated carbon plume flow dynamics under magnetic field. *J. Appl. Phys.* **105**, 084909.
- SEMEROK, A., FOMICHEV, S.V., WEULERSSE, J.-M., BRYGO, F., THRO, P.Y. & GRISOLIA, C. (2007). Heating and ablation of Tokamak graphite by pulsed nanoseconds ND-YAG lasers. *J. Appl. Phys.* **101**, 084916.
- SIZYUK, V., HASSANEIN, A. & SIZYUK, T. (2006). Three-dimensional simulation of laser-produced plasma for extreme ultraviolet lithography applications. *J. Appl. Phys.* **100**, 103106